

Article

# Advances in the Coastal and Submarine Groundwater Processes: Controls and Environmental Impact on the Thriassion Plain and Eleusis Gulf (Attica, Greece)

Demetrios Hermides <sup>1,\*</sup> , Panayota Makri <sup>2</sup>, George Kontakiotis <sup>2</sup>  and Assimina Antonarakou <sup>2</sup>

<sup>1</sup> Department of Natural Resources Management and Agricultural Engineering, Agricultural University of Athens, 11855 Athens, Greece

<sup>2</sup> Faculty of Geology & Geoenvironment, Department of Historical Geology-Paleontology, School of Earth Sciences, National & Kapodistrian University of Athens, Zografou University Hill, 15774 Athens, Greece; pmakri@geol.uoa.gr (P.M.); gkontak@geol.uoa.gr (G.K.); aantonar@geol.uoa.gr (A.A.)

\* Correspondence: dermidis@aua.gr

Received: 30 September 2020; Accepted: 16 November 2020; Published: 20 November 2020



**Abstract:** This study focuses on the hydrogeological conditions in the coastal (Thriassion plain) and submarine (Eleusis Gulf) environment of West Attica, Greece. Up to now, the predominant aspect for the Thriassion plain groundwater—hosted within the Neogene-Quaternary sediments—was its direct hydraulic contact with the seawater. Due to that, the coastal plain groundwater is strongly believed to be of brackish quality irrespective of the local hydrodynamic conditions. Our major goal is to evaluate the actual mechanism controlling the groundwater flow, the origin and distribution of saline water, and the existence of fresh groundwater in the submarine environment. We summarize the following: (1) groundwater of the Thriassion plain is partly discharged as an upwards leakage from deeper aquifers, (2) modern direct seawater intrusion is not possible in the Neogene-Quaternary sediments, and (3) fresh groundwater possibly exists below the sea floor of the Eleusis Gulf. The results may serve as hint of further research in groundwater resources below the Mediterranean Sea floor, and, consequently, a new perspective on water resource management could emerge.

**Keywords:** offshore groundwater exploration; coastal aquifers; salt-/fresh-water relationship; Mediterranean Sea; Attica-Greece

## 1. Introduction

The sustainable management of coastal aquifer resources requires a good understanding of the relationship between salt and fresh water. Coastal aquifers have been extensively studied for more than a century by many researchers [1–18]. The common problem in coastal aquifers, which are hydraulically connected to the sea, is seawater intrusion mainly, but not exclusively, due to overpumping. Overpumping forces the salt-fresh water interface shift landward, resulting in the contamination of the fresh groundwater with seawater. This phenomenon is depended on (i) the geological-hydrogeological and hydraulic characteristics of the aquifer, (ii) human activities, and (iii) tidal effects and coastal and sea bottom conditions [5]. The hydrostatic equilibrium (Figure 1a) between salt and fresh water is described by the Ghyben-Herzberg principle, Equation (1):

$$z = \frac{\rho_f}{\rho_s - \rho_f} h_f \quad (1)$$

where  $z$  = is the depth to the salt-fresh water interface below sea level,  $h_f$  = is the height of the fresh water above sea level,  $\rho_s$  and  $\rho_f$  = salt-water and fresh-water densities, respectively, and  $g$  = acceleration due to gravity.

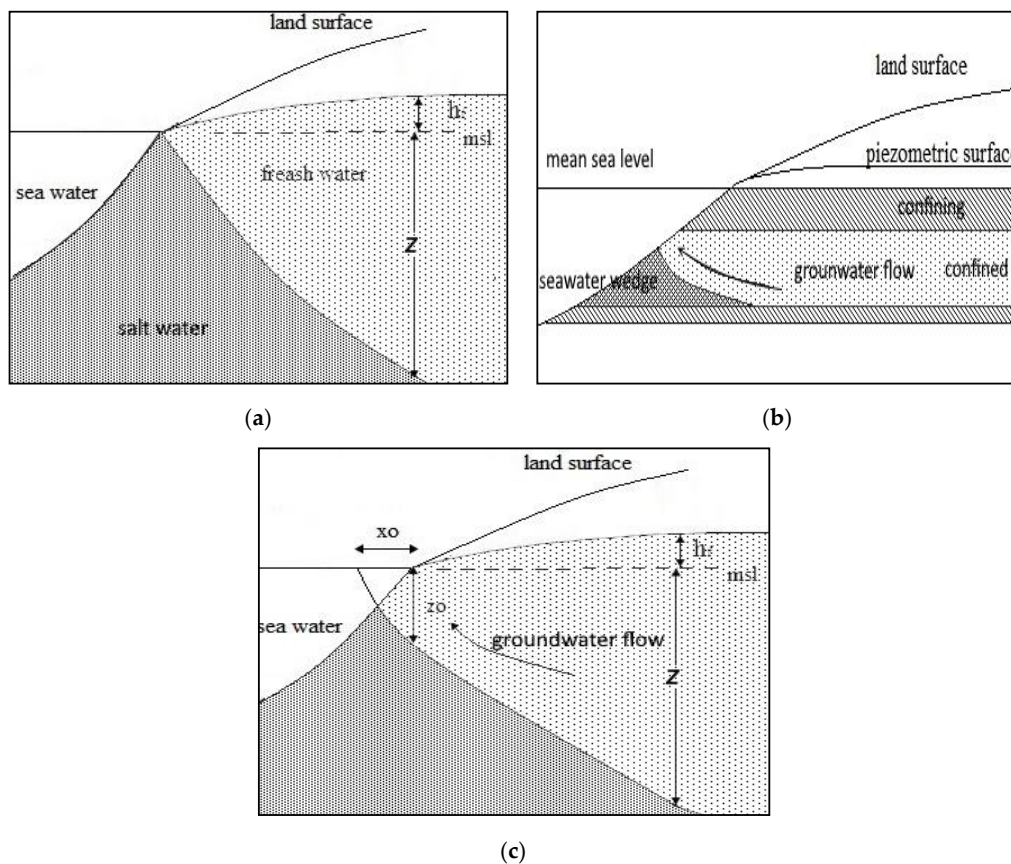


**Figure 1.** Dupuit-Ghyben-Herzberg model flow (a) in unconfined and (b) confined coastal aquifers, and the (c) actual groundwater discharge onto the sea floor;  $z$  is the depth to the salt-fresh water interface below sea level,  $h_f$  is the height of the fresh water above sea level,  $x_0$  is the width of the submarine zone through fresh groundwater discharge into the sea, and  $z_0$  the depth of the interface below the coastline.

In ideal conditions, the Ghyben-Herzberg principle states that the depth to the salt-fresh water interface  $z$  beneath sea level is approximately 40 times the height  $h$  of the fresh water above sea level. The application of the above principle is limited to conditions in which the two liquids are static, and it is valid under the occurrence of horizontal groundwater flow. It can be also applied in unconfined and confined aquifers (Figure 1b).

Based on the Dupuit–Forchheimer assumption that, in coastal aquifers, the equipotential lines are vertical (horizontal flow) in combination with the Ghyben-Herzberg principle, a one-dimensional flow can be used that yields the following expression for the  $x$  and  $z$  coordinates of the interface [2].

$$z^2 = \frac{2\rho_f q' x}{\Delta\rho K} \tag{2}$$

where  $q'$  = fresh groundwater outflow at the coastline per unit width,  $K$  = the hydraulic conductivity, and  $\Delta\rho$  = the difference of the salt- and fresh-water densities.

Based on Glover’s analytical solution [12], Cheng and Quazar [16] determined the interface depth as:

$$z^2 = \frac{2\rho_f q' x}{\Delta\rho K} + \left(\frac{\rho_f q'}{\Delta\rho K}\right)^2 \tag{3}$$

where  $K$  = the hydraulic conductivity.

The width  $x_0$  (Figure 1c) of the submarine zone through fresh groundwater discharge into the sea can be obtained from Equation (3) by setting  $z$  equal to 0, which provides Equation (4), and the depth of the interface below the coastline  $z_0$  by setting  $x$  equal to zero, which provides Equation (5).

$$x_0 = \frac{\rho_f q'}{2\Delta\rho K} \quad (4)$$

$$z_0 = \frac{\rho_f q'}{\Delta\rho K} \quad (5)$$

In real field conditions, this interface does not occur; instead, a brackish transition zone exists where complex diffusion and mass transport theories are developed [19,20]. The overexploitation of coastal groundwater leads to both submarine groundwater discharge reduction, as well as an increase of seawater inflow and, consequently, an increase of the transition zone thickness [21].

Coastal aquifers, which are in hydraulic contact to the sea, are subject to fluctuations in the hydraulic head due to the tides [22]. The fluctuation parallels to the rise or fall of the tides after a time lag between the high tide and the peak of the groundwater level.

On the contrary, in confined aquifers extending below the sea floor without a sea front and which are separated from seawater by thick confining layers of very low permeability, fresh groundwater can be conserved against salinization. Identical geological-hydrogeological structures exist in many places all over the world, such as The Netherlands [1]; Eastern England [5]; Spain [20]; the Bay of Bengal; Bangladesh [23]; the USA [2,24]; and Estonia, Denmark, and France [25]. Thus, the boundary between the aquifer and seawater does not exist, or it migrates far from the coast. Therefore, the Ghyben-Herzberg seawater-fresh water interface does not occur near the coast. In these aquifers, fresh groundwater occurs beneath the sea floor fed from the onshore outcrops [1,2,4,24–27]. Offshore groundwater occurrence is a global phenomenon, but its direct observations are limited. The assessment of groundwater fluxes into the sea, or the submarine aquifers often need specific techniques and procedures, as well [28]. However, at many regions, onshore hydrogeological and hydrochemical data provide strong indirect evidence for the occurrence of fresh groundwater in submarine aquifers below the sea floor [25].

In this article, the functioning of the Thriassion Plain coastal aquifers was completely revised, and an attempt to evaluate the actual mechanism controlling the groundwater flow, the origin and distribution of saline water, and the existence of fresh groundwater in the submarine environment of the Eleusis Gulf in the East Mediterranean was made

## 2. Study Area

The Thriassion Plain is a coastal area of about 120 km<sup>2</sup> in extent (Figure 2) and lies from latitude 38.0 and 38.2° N and longitude 23.1 to 23.7° E. It is part of three hydrological basins of 475 km<sup>2</sup> in total extent. The plain is surrounded by the Mesozoic carbonate, which drains south into the Eleusis Gulf. A semiarid climate prevails in the area. The annual precipitation is around 380 mm/y, while the actual evapotranspiration is around 62% of the precipitation [29]. The mean groundwater temperature is 20.6°, which ranges between 17.5 and 22.8 °C [29]. The mean air temperature ranges between 9.2–29.9 °C in January and July, respectively. The mean sea surface temperature of the Eleusis Gulf ranges between 13 and 25 °C, while the mean sea temperature at the bottom of the Eleusis Gulf ranges between 12 and 13 °C. The Eleusis Gulf is a small and almost enclosed sea north of the Saronikos Gulf in the East Mediterranean Sea, which covers an area of 67 km<sup>2</sup>, having a maximum depth of 33 m. It is surrounded by the study area to the north and the Salamis Island to the south. Its connection to the Saronikos Gulf is through two shallow channels of 8 m in depth at the western end and 12 m in depth at the eastern end, respectively. This area has been degraded environmentally due to uncontrolled agricultural and industrial development during recent decades [30–33].

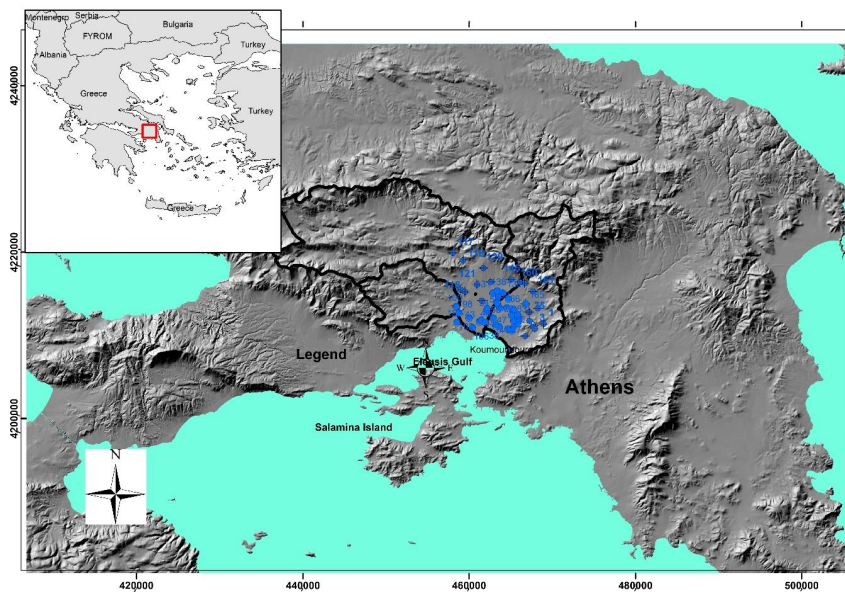


Figure 2. Study area.

### 3. Regional Setting

#### 3.1. Geological Setting

The Thriassion Plain is located at the border between non-metamorphic and metamorphic rocks of Eastern Greece and Attica geotectonic units, respectively [34]. The geological structure (Figure 3) of the study area consists of: (1) a Palaeozoic volcano-sedimentary complex, 400–500-m thick, composed of: (a) clastic materials (arkoses, greywackes, shales in alternations with phyllites, conglomerate, and lenticular intercalations of limestone) and (b) basic-igneous volcanic rocks; (2) Mesozoic sediments consisting of: (a) Lower-Middle Triassic phyllites and sandstones with breccia-conglomerate intercalations; (b) volcanic rocks and tuffs; (c) Middle-Upper Triassic white carbonate, crystalline in places, comprising limestone, dolomitic limestone, and dolomite; (d) Upper Triassic black limestone, dolomitic limestone, and (e) Grey Cretaceous limestone; and (3) Cenozoic sediments of: (a) Neogene (Pliocene marls with lignite intercalations in places, clay, conglomerate, sandstone, and marly limestone); (b) Pleistocene deposits (clay, sand, gravel, and torrential fans of loosely and cohesive conglomerate); and (c) Holocene deposits (clay, loam, sand, and gravel) [35].

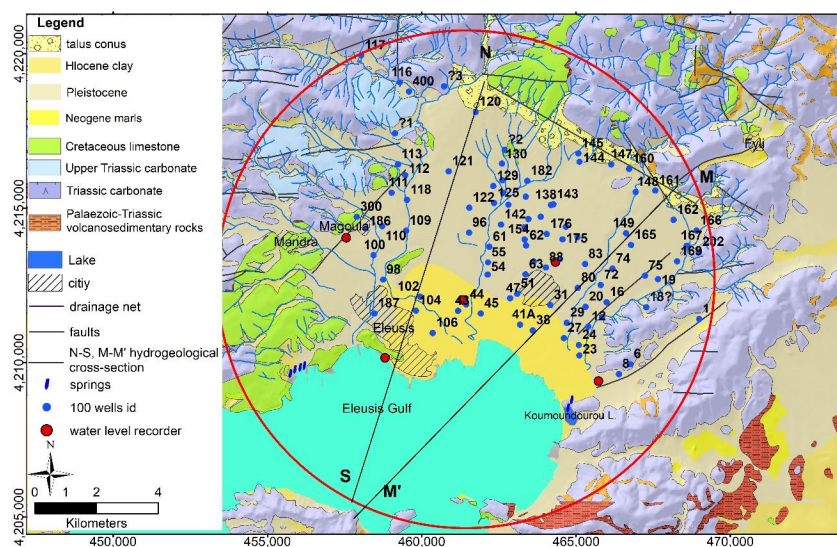


Figure 3. Geological map of the study area. The numbering is the wells id.

### 3.2. Structural and Lithostratigraphic Setting

The lithostratigraphic setting of the plain comprises sediments of the Plio-Pleistocene and Holocene ages. East of the study area, this sequence is underlain by marls. Marly limestone and marls have been found in some wells NE of Aspropyrgos City at depths between 63–71 and 96–170 m from the ground surface, respectively [36,37]. Cretaceous limestone and Triassic carbonate occur at the depths of 20–40 and 80–100 m from the ground surface, respectively, N of Eleusis City. Arkoses, greywackes, and shales of the Palaeozoic age have been found NE and SE of the study area in alternations with phyllites.

The Thriassion Plain was influenced by tectonic factors during the Neogene-Quaternary [34,35,38–40]. The Triassic carbonate is massive in a large extent, and, in some places, it is karstified, depending on the extent to which it has been affected by karstification and/or tectonism. During Pliocene and Pleistocene, intense tectonic actions created horsts and grabens (Figure 4). Geophysical research carried out in the area by [38] showed that the Mesozoic basement is not found to the depth of 320–450 m at the central part of the plain. The study area has been influenced by Pleistocene sea level changes, as well [41–44].

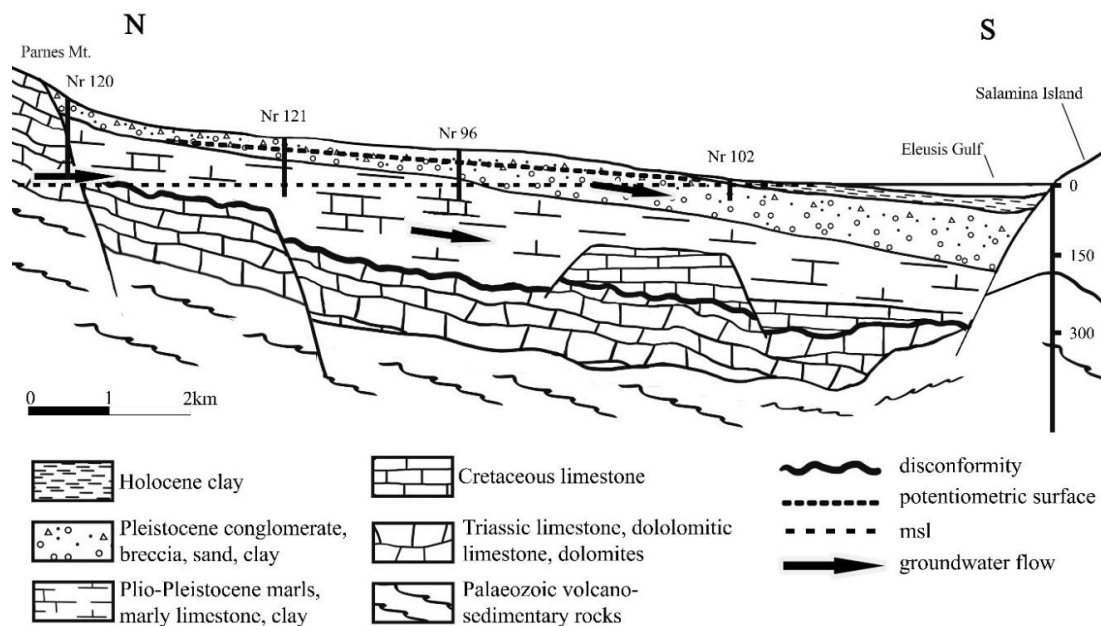


Figure 4. Geological-Hydrogeological cross-section of the N-S direction.

### 3.3. Hydrogeological-Hydrochemical Setting

The history of pumping started in 1900. Since then, brackish water has been found in the upper aquifers [45]. Some wells located west of the plain were connected by galleries, resulting in expanding the contamination of fresh water with brackish water. In order to study the origin of the saline water, the Institute for Geological and Underground Research monitored the tidal change impacts on the Thriassion aquifers [46]. Five automatic recording devices were placed more than a year at the study area. One device was placed in the Eleusis Gulf to monitor tidal changes. One device was placed at the Holocene sediments 1 km from the shoreline, while two of them were placed at the Pleistocene deposits 2 and 3 km far from the shore; the last one was placed in the Triassic carbonate 3.5 km from the shore north of Eleusis City. No influence of tidal changes was recorded on the Pleistocene-Holocene aquifers; instead, influence was observed in the borehole drilled in the Triassic aquifer. Groundwater response was 2 cm after a time lag ( $t_{lag}$ ) between the high tide and the peak of the groundwater level,  $t_{lag} = 36$  h. Tidal period was 24 h, and the tidal amplitude was 8 cm. The hydrogeological conceptual model that was proposed so far [30,46–48] suggested the existence of two unconfined aquifers in the plain: (i) the upper one, which occurs in the Pleistocene-Holocene deposits, and (ii) the lower one in the Mesozoic carbonate rocks, which both discharge at the shoreline of Aspropyrgos and Eleusis Cities.

A mathematical model, based on the previous conceptual model, failed to describe the hydrogeological regime of the plain.

Saline water in the plain aquifers is limited to a zone of 2 to 3 km in width from the shoreline. The Na/Cl molar ratio is between 0.73–0.87, and the chlorides are between 12–205 mmol/L. In the western, eastern, and the northern parts of the study area where carbonate outcrops, saline groundwater was found 8 to 9 km inland, with total dissolved solids (TDS) between 1500–6000 mg/L and the chlorides between 15–90 mmol/L [29–33,46–49]. Groundwater flows SW with hydraulic gradient 1‰. Transmissivity (T) in the Cretaceous aquifer is around 5000 m<sup>2</sup>/d (0.5787 m<sup>2</sup>/s) [48]. During the last five decades, due to the heavy pumping in the Plio-Pleistocene aquifers, at the central part of the basin, the dynamic level was lowered below sea level; however, the static level fluctuated between 5 m below sea level and 3 m above sea level, and groundwater of good quality (TDS values between 400–1200 mg/L and chlorides between 1–9 mmol/L) was preserved for a long time, despite the overpumping conditions [40,46–50].

Studies on the Eleusis Gulf seawater [51,52] presented data on its temperature, salinity, dissolved oxygen (DO), and inorganic nutrients. Both the studies were in accordance with each other. It was also reported [51,52] that the temperatures of the water at 1, 10, 20, and 30 m in depth remain stable at 12.5 °C in January and fluctuate between 12.5 and 17 °C in May. Salinity fluctuates between 38.3 and 38.5‰ in January and 38.2–38.5‰ in May [51].

#### 4. Materials and Methods

Lithostratigraphic cross-sections from boreholes drilled in the Thriassion Plain during 1952–2007 by the Land Reclamation Service of Agricultural Ministry (LRSAM) were taken into consideration. Water samples from 45 wells were collected in June 2012. Electric Conductivity (EC) and pH were measured in situ on the head of the pumping column (HACH). The samples were analyzed in the laboratory of Mineralogy and Geology in the Agricultural University of Athens. The average analytical precision was better than 5%. Ion chromatography (Metrohm 732) was used for major component determination, and the method of titration was used in determination of HCO<sub>3</sub><sup>-</sup>. Water level was measured carefully 2–5 times/year for a 15-year period from 1999–2014 in 48 wells. Additionally, pumping tests in 7 agricultural large-diameter wells were carried out in the Plio-Pleistocene deposits during the 2009–2012 time period.

#### 5. Results and Discussion

The study on the LRSAM data showed that the water level in most wells stood above the top of the aquifers as high as 1–5 m during the drillings phase. In addition, the monitoring of the water level, as well as the analysis and evaluation of the pumping test data, concluded that the larger part of the aquifers is confined and semi-confined. Hydrochemical data (Tables 1–3) of the onshore groundwater indicate that fresh groundwater is possibly hosted in the offshore submarine aquifers. The Pleistocene-Holocene clay layers occur very frequently in different depths from 0–170 m throughout the plain in alternations with gravel, sand, and conglomerates 2–10 m in thickness. This Pleistocene-Holocene sequence being partly of shallow marine, partly of terrestrial origin contains the coastal aquifers. Clay typically ranges from 0.5 m to 80 m in thickness.

Based on their hydrogeological and geological-lithostratigraphic characteristics, the aquifers are grouped into three hydrostratigraphic units (HSU): the Neogene-Quaternary unit, the Cretaceous, and the Triassic one. The first one is divided into the Plio-Pleistocene subunit, which is under confined conditions, and the Holocene-Pleistocene subunit, which is confined/semi-confined and locally unconfined.

**Table 1.** Hydrogeological and hydrochemical data from the wells of the Triassic HSU. TDS: total dissolved solids.

HSU	Well Nr	Distance from Shore (m)	Site Elevation (m)	Well Depth (m)	Head (masl)	TDS (mg/L)	Cl <sup>-</sup> (mmol/L)	Na <sup>+</sup> (mmol/L)	Ca <sup>2+</sup> (mmol/L)	Mg <sup>2+</sup> (mmol/L)	K <sup>+</sup> (mmol/L)	NO <sub>3</sub> <sup>-</sup> (mmol/L)	SO <sub>4</sub> <sup>2-</sup> (mmol/L)	HCO <sub>3</sub> <sup>-</sup> (mmol/L)
Triassic carbonate	6	2559	50	60		2074	21.7	20.8	7.7	6.2	0.5	0.8	2.7	6.9
	18	4000	58	60		2476	29.9	23.8	7.4	6.6	0.5	0.4	2.5	7.8
	111	5041	63.5	85		1463	16.4	12.0	6.6	4.4	0.2	0.6	1.4	5.5
	121	5496	74			412	1.1	1.0	2.7	2.9	0.0	0.6	0.2	4.0
	169	5690	69.51	85		1731	11.7	10.8	7.5	5.0	0.3	0.5	1.2	9.2
	202	6080	76.5	80	6.17									
	147	6735	140	137		1259	12.3	10.7	4.5	3.6	0.5	0.2	2.3	5.0
	162	6800	140	140		354	1.0	1.0	2.7	2.1	0.0	1.1	0.3	3.3
	116	8625	115	154	13.63	900	7.2	5.8	5.9	3.0	0.2	0.6	0.9	5.0
	117	9410	175	220	12.63	950								

**Table 2.** Hydrogeological and hydrochemical data from the wells of the Cretaceous HSU.

HSU	Well Nr	Distance from Shore (m)	Site Elevation (m)	Well Depth (m)	Head (masl)	TDS (mg/L)	Cl <sup>-</sup> (mmol/L)	Na <sup>+</sup> (mmol/L)	Ca <sup>2+</sup> (mmol/L)	Mg <sup>2+</sup> (mmol/L)	K <sup>+</sup> (mmol/L)	NO <sub>3</sub> <sup>-</sup> (mmol/L)	SO <sub>4</sub> <sup>2-</sup> (mmol/L)	HCO <sub>3</sub> <sup>-</sup> (mmol/L)
Cretaceous limestone	96	3460	38	76	4.8	1980	21.1	16.4	6.1	9.3	0.4	1.0	1.8	8.3
	118	4938	64	80		2695	36.5	28.1	7.2	7.3	0.5	0.4	3.1	5.6
	130	5697	81.35	95		1452	16.5	11.8	8.2	5.3	0.1	2.3	2.7	3.7
	120	7303	145	180		2044	27.1	20.9	5.3	5.4	0.4	0.2	2.1	5.0



Table 3. Cont.

HSU	Well Nr	Distance from Shore (m)	Site Elevation (m)	Well Depth (m)	Head (masl)	TDS (mg/L)	Cl <sup>-</sup> (mmol/L)	Na <sup>+</sup> (mmol/L)	Ca <sup>2+</sup> (mmol/L)	Mg <sup>2+</sup> (mmol/L)	K <sup>+</sup> (mmol/L)	NO <sub>3</sub> <sup>-</sup> (mmol/L)	SO <sub>4</sub> <sup>2-</sup> (mmol/L)	HCO <sub>3</sub> <sup>-</sup> (mmol/L)
Unconfined Holocene-Pleistocene subunit	41	800	8.81	15	3.03	1683	10.4	16.8	5.8	5.1	0.1	2.9	2.8	9.9
	38	872	9.3	11	2.58	2337	26.4	18.1	11.1	8.6	0.3	1.2	3.9	7.3
	45	883	4.72	6.2	1.9	4318	59.5	48.4	10.9	12.4	0.7	6.7	6.6	6.3
	106	1010	5.91	8.5	0.96	3243	40.8	32.5	11.1	9.5	0.5	1.5	4.8	7.4
	187	1100	13.02	14	3.85	1406	15.6	12.4	4.7	4.5	0.4	0.4	1.4	5.4
	43	1156	5.1	5.93	1.8	2184	27.7	25.1	4.7	5.9	0.6	2.5	2.6	5.1
	47	1200	10.5	11.93	1.64	5026	80.7	34.6	24.8	26.8	0.6	3.5	4.6	4.5
	44	1222	7.51	9.8	2.52	1298	12.2	12.9	3.2	3.7	0.4	0.2	1.4	6.1
	27	1423	16.36	16	3.79	2608	29.2	27.7	9.3	7.5	0.4	0.8	4.0	7.2
	98	2200	25.98	32	5.26	1108	6.9	6.5	6.2	4.1	0.3	0.6	1.4	7.5
	102	2228	14.39	20	3.13	2395	26.0	22.9	7.6	8.5	0.4	2.5	3.0	8.5
	14	2601	28	30	4.68	3161	42.1	27.5	15.2	10.3	0.3	2.7	5.1	5.3
	100'	2945	33.9	35	9.36									
	154	3424	46.62	65	6.3	646	2.7	1.8	6.6	6.2	0.2	5.6	1.0	4.0
	72	3469	50.88	60	6.88	889	7.0	3.6	6.2	6.0	0.2	2.1	0.9	5.0

### 5.1. The Neogene-Quaternary Hydrostratigraphic Unit

The Holocene sediments, mainly made up of clay and sandy clay five m in thickness, confine the underlying Late-Pleistocene aquifer. Locally, in palaeovalleys and/or sandy parts of the deposits, the aquifer is unconfined (wells # 38, 41, 43, 45, and 47). The depth of the wells is 3–10 m. The annual head fluctuation ranges from 0.15–0.48 m. In general, they exhibit upwards leaky conditions, which form swamps and marshes in many sites on the ground. At the Kalimbaki site, artesian wells (or once artesian) onto the ground surface, as well as manifestations of surface water, such as springs, lakes (e.g., Koumoundourou Lake), or marshes on the coastal area of Eleusis and Aspropyrgos Cities, could betoken part of groundwater discharge of either the Quaternary aquifers or the Triassic carbonate. Salinization of the water may have taken place due to (i) the dissolution of evaporite relics, (ii) evaporation of the irrigation water, and (iii) farms and domestic sewage [50]. It is also very likely that salinization took place during the Holocene transgression or/and due to the presence of connate water from the contemporary deposition of clay during the transgressions. Taking into account that (i) groundwater is not subject to hydraulic head fluctuations caused by the tides of the sea, (ii) there is an upwards leakage at many sites on the ground of the coastal area, (iii) the occurrence of Holocene clay, which probably continues below the sea bottom and prevents seawater directly intruding through the clay, and (iv) the hydraulic head is above sea level; it is considered that groundwater is not in hydraulic contact to the sea, and, finally, modern direct seawater intrusion in Holocene sediments is not possible.

Pleistocene sands, gravels, clay, or conglomerates are under confined conditions, as well. In this strata sequence, up to six aquifers are developed 2–10 m in thickness (Figure 5) at depths 20–140 m from the ground surface. Plio-Pleistocene marls, marly limestone, sandstone, clay, and conglomerates form a confined aquifer that reaches up to 90 m below the sea level.

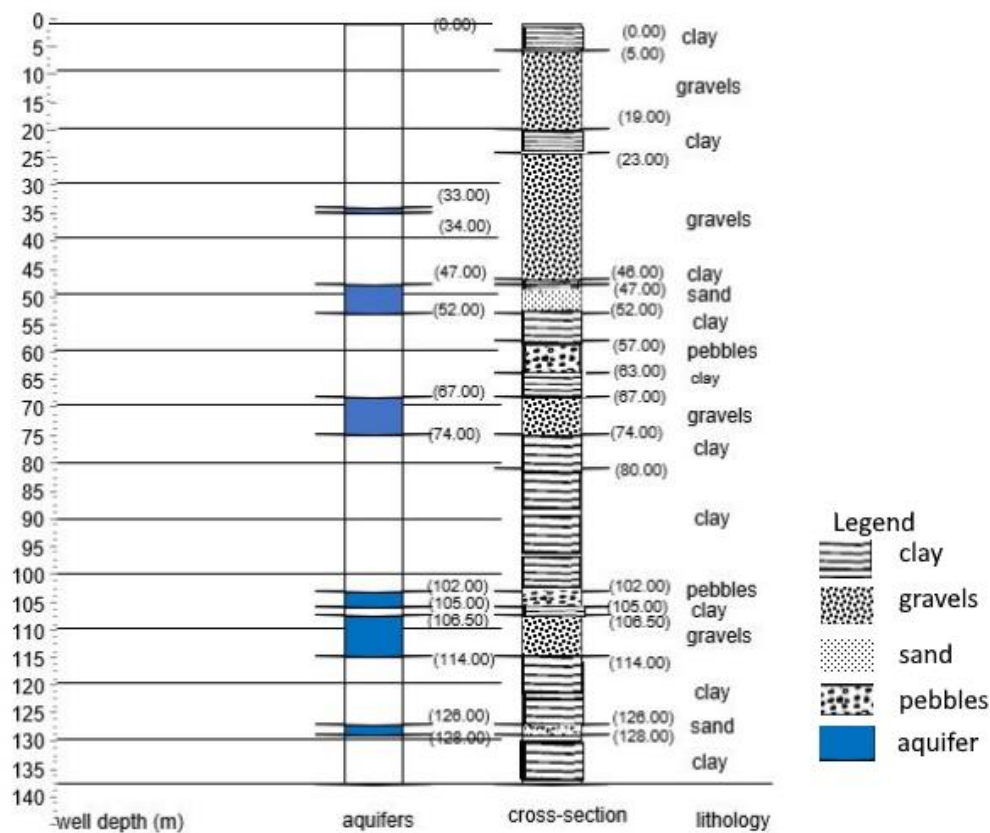
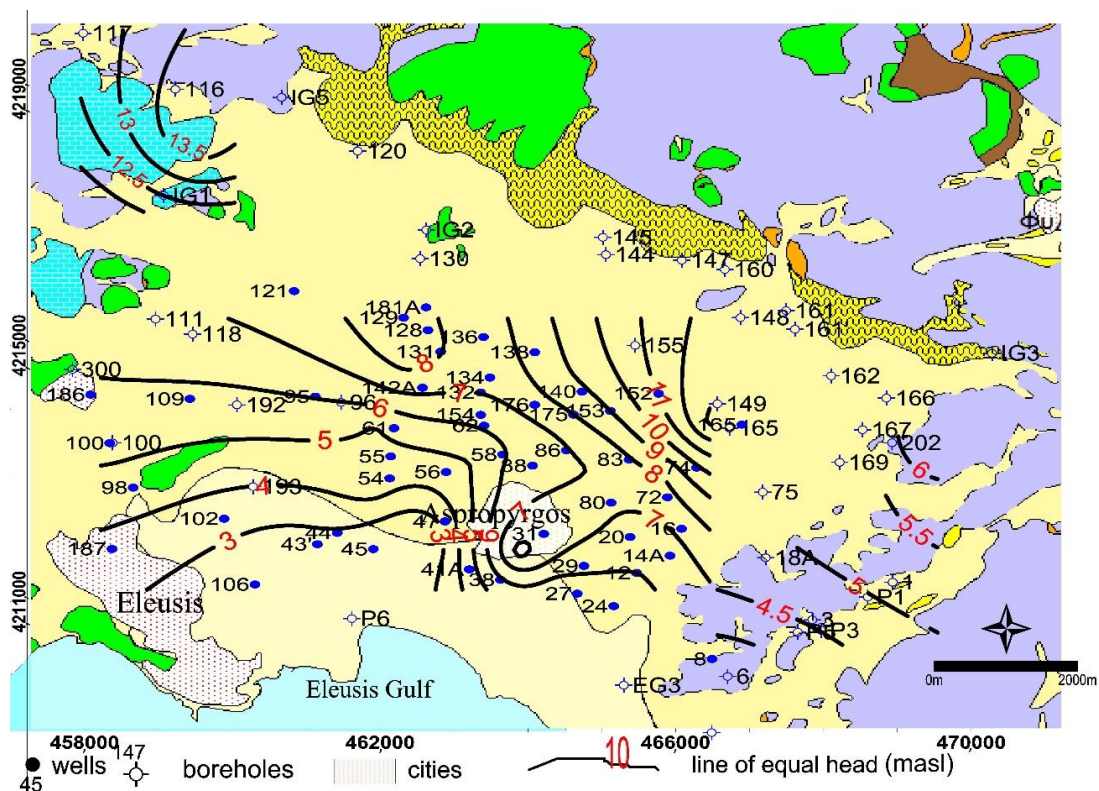


Figure 5. Geological-Hydrogeological characteristics of the wells in the Thriassion Plain.

Pumping tests carried out in the wells # 54, 86, 128, 129, 131, 154, and 154P2 in the Pleistocene sediments were analyzed and evaluated for both confined and unconfined aquifers, using mainly unsteady-state flow methods [53–56] and recovery methods. Drawdown after 6–12 h of pumping was 0.86, 1.11, 5.24, 9.74, 4.66, 1.31, and 1.26 m, respectively. The Schafer equation [57], which provides an estimation of time  $t_c$  at which the casing storage effect is negligible, was applied, as well. The analysis showed that the hydraulic characteristics of the wells were variable, depending on the sedimentation material that the aquifer was made up. Transmissivity  $T$  ranged from 3.5–275 m<sup>2</sup>/d ( $4 \times 10^{-5}$ – $3 \times 10^{-3}$  m<sup>2</sup>/s), storativity  $S$  ranged from  $1.75 \times 10^{-3}$ – $8.9 \times 10^{-3}$ , and hydraulic conductivity  $K$  ranged from 0.4–25 m/d ( $4.6 \times 10^{-6}$ – $3 \times 10^{-4}$  m/s). The Pleistocene sediments are confined (dug wells 29, 31, 54, 58, 61, 74, 83, 128, 129, 131, 132, 134, 136, 140, 142, 175, and 176 and boreholes 75, 100, and 138) or semi-confined (12, 16, 20, 24, 44, 31, 54, 55, 62, 80, 86, 88, 109, 121, 165, 181, and 186), and, in some wells, unconfined aquifers are developed (dug wells 14, 27, 41, 43, 45, 47, 72, 98, 100', 102, 106, 154, and 187). The annual head fluctuation ranges between 1.43–2.40 m in the confined aquifer, 0.63–1.22 m in the semi-confined, and 0.36–0.58 m in the unconfined one. The head in the unconfined aquifer is between 1 and 34 masl and, in the confined/semi-confined system, is up to +9 masl. Figure 6 shows the hydraulic head in the Thriassion Plain aquifers in March 2014. An almost stagnant zone is developed under the coastal area, where the minor discharge occurs as an upwards leakage through the aquitards, forming wetlands or swamps on the ground surface. Groundwater discharge into the sea is negligible, as the seawater salinity and the temperature at the bottom of the Eleusis Gulf remained at 38.3‰ and 12.5 °C for many years [51,52]. It is very likely that the groundwater is prevented from progressing further beneath the seafloor due to the barrier of the Salamina Island and, therefore, moves very slowly eastwards.



(a)

Figure 6. Cont.

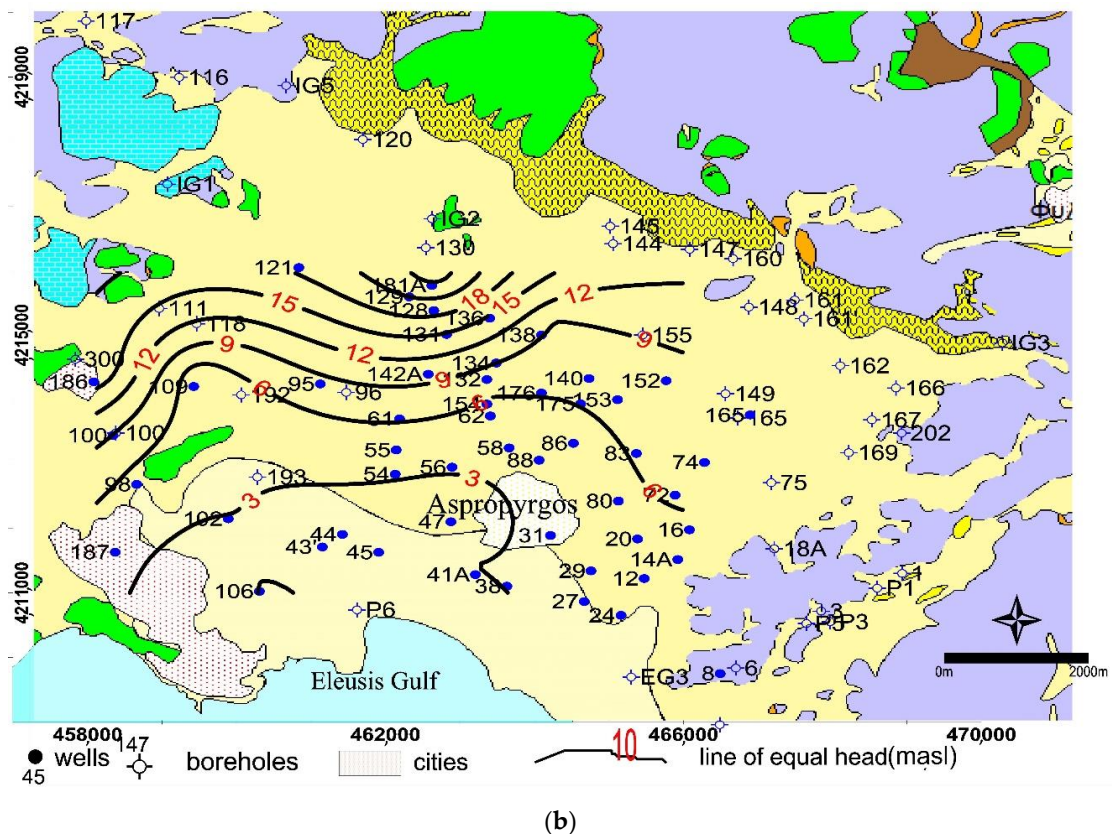
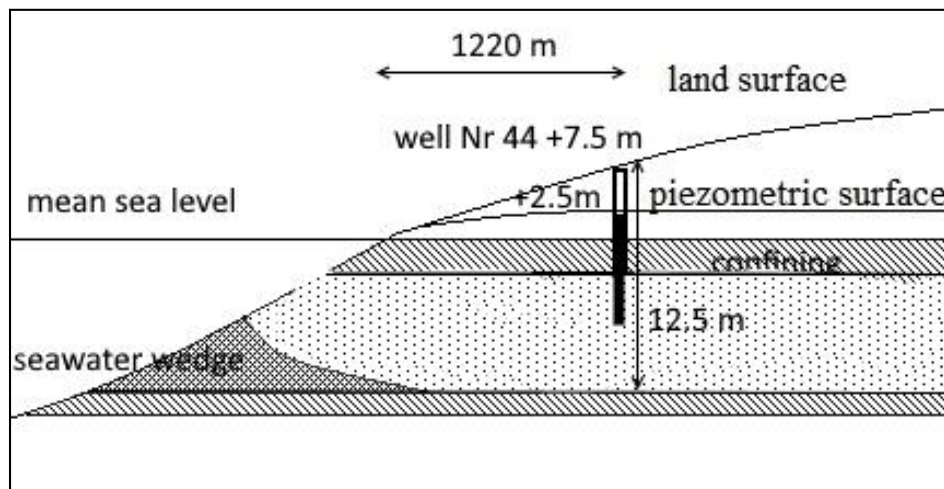


Figure 6. Potentiometric surface. (a) Triassic-confined and Triassic-unconfined Pleistocene aquifers and (b) a Holocene unconfined aquifer.

It was observed that confined aquifers turned into unconfined ones in the wells # 181 and 129 and 136, 62, and 165 under overpumping conditions, with a drawdown around 30 m and 20 m from the original static level, respectively. In the wells # 62, 131, 134, 136, 138, 140, and 154 located at the central part of the basin, the water level stands below the sea level during pumping without deteriorating the water quality;  $Cl^-$  ranges between 1.2 and 8.1 mmol/L and EC between 810 and 1586  $\mu S/cm$ . Despite the increased drawdown by heavy pumping the last 50 years, the static level is still above the sea level. Combined with the presence of good water quality, which occurs in the central part of the plain, as well as the limited contaminated with seawater coastal zone up to 2 to 3 km in width for at least 100 years, it is deduced that seawater cannot intrude inland further. It is very likely that the thick clay layers of the Pleistocene age extend under the sea bottom, and the multi-layered aquifer system occurs beneath the seafloor, as well; therefore, there is no vertical or another boundary of the multi-layered system with the seawater. Consequently, the Plio-Pleistocene aquifers are not in direct contact with the sea.

Trying to determine a salt-freshwater interface, in the first calculations, consider the well # 44 located 1220 m far from the shoreline tapping the Pleistocene confined aquifer with a thickness of 5 m (Figure 7). The site altitude is 7.51 masl, and the well depth is 9.8 m (-2.29 mbsl). The hydraulic gradient is 0.001, and the head is 2.5 masl. It is also assumed that  $T = 200 \text{ m}^2/d$ ; thus,  $q' = T \times i = 200 \times 0.001 = 0.2 \text{ m}^2/d$  and  $k = 200/5 = 40 \text{ m/d}$ . Then, the depth to the interface at well # 44 based on Equation (2) where no vertical flow occurs is  $z = (2 \times 40 \times 0.2 \times 1220 / 40)^{0.5} = 22 \text{ m}$ . In this case, seawater could not intrude into well 44, since the depth to the interface exceeds the aquifer thickness; therefore, the seawater wedge is missing [2]. In addition, based on Equations (4) and (5), the depth to the interface at the shoreline is  $z_0 = 40 \times 0.2 / 40 = 0.2 \text{ masl}$ , and the width of the outflow face  $x_0 = 40 \times 0.2 / 40 = 0.1 \text{ m}$ . Sources of uncertainty to calculate the groundwater flux and the depth to the interface could be the hydraulic

( $K$ ,  $q'$ , and  $i$ ) and geometric (thickness and slope) characteristics of the aquifer. Homogeneity of the aquifer is also the source of uncertainty.



**Figure 7.** High salinity of groundwater in well Nr 44 could not be attributed to modern direct seawater intrusion, as the salt-freshwater interface is missing.

The hydrochemical data from such wells, as it is reported in the hydrochemical settings section, show that groundwater in the coastal area of about 2 to 3 km in width was found brackish during the drilling phase. This means that seawater intruded inland in a past geological time due to Pleistocene seawater fluctuations [17] or that it is entrapped (palaeo)seawater. Groundwater quality due to repeated irrigations with brackish water and the high evapotranspiration that is around 62% of the precipitation made the water quality worse, which led to high values of salinization.

### 5.2. The Cretaceous Unit

The Cretaceous limestone hosts an unconfined aquifer (# 111, 120, and 130) with a hydraulic head up to +8 masl. The water table annual fluctuation is around 0.60 m. Hydrochemical data indicate that Cretaceous limestone is contaminated with seawater. Chlorides range from 16.4–36.5 mmol/L and sodium from 11.8–28.1 mmol/L; the sodium/chloride molar ratio ranges from 0.72–0.77. In this aquifer, passive seawater encroachment could take place, which means that the head is above sea level, and groundwater still flows seawards. However, as the water was found brackish since the early 1950s, seawater intrusion seems to be happened in a previous geological time. Due to the Pleistocene sea level rise and, mainly, the last 12 ka and the fact that limestone is intensively fractured, the seawater intruded 9 km inland.

### 5.3. The Triassic Unit

The Triassic carbonate west and north of the study area is under confined conditions in massive limestone-dolomite (wells # 116, 117, 147, and 162), and it is unconfined in karstified and intensely fractured limestone-dolomitic limestone (wells # 6, 18, 169, and 202), with a hydraulic gradient 0.5–1‰ SW seawards. Transmissivity  $T$  ranges from 15–350 m<sup>2</sup>/d ( $1.74 \times 10^{-4}$ – $4.1 \times 10^{-3}$  m<sup>2</sup>/s). TDS ranges between 900–3000 mg/L. The confined units appear to maintain their fair quality with TDS between 400–1400 mg/L; instead, in the karstified units, the TDS is up to 2500 mg/L. The seawater front has intruded 8 to 9 km inland. Brackish water with EC = 14,000  $\mu$ S/cm has been found 10.5 km inland [36].

Trying to determine a salt water-fresh water interface, it is assumed the presence of two wells, A and B, located 8000 m and 10 m from the shoreline are tapping the Triassic aquifer, which has a saturated thickness of 50 m. It is also assumed that  $T = 300$  m<sup>2</sup>/d and  $I = 0.001$ ; thus,  $q' = T \times i = 300 \times 0.001 = 0.3$  m<sup>2</sup>/d and  $k = 300/50 = 6$  m/d. Then, the depth to the interface ( $i$ ) at well A based on Equation (2), where no

vertical flow occurs, is  $z = (2 \times 40 \times 0.3 \times 8000/6)^{0.5} = 179$  masl and, (ii) at well B based on Equation (3), where vertical flow occurs, the depth to the interface is  $z = (2 \times 40 \times 0.3 \times 10/6 + (40 \times 0.3/6)^2)^{0.5} = 6.63$  m. In addition, based on Equations (4) and (5), the depth to the interface at the shoreline is  $z_0 = 40 \times 0.3/6 = 2$  masl, and the width of the outflow face  $x_0 = 40 \times 0.3/(2 \times 6) = 1$  m, respectively.

The hydrochemical data from such wells as it is reported in the hydrochemical settings section show that groundwater was found brackish during the drilling phase. This means that seawater intruded inland in a past geological time, probably due to Pleistocene seawater fluctuations, or that it is fossil or entrapped (palaeo)seawater.

In recent years, water samples from wells # 54, 41, 83, 86, 16, 98, and 27 in the Pleistocene deposits show that EC values and chloride concentrations have spectacularly been reduced. On the contrary, in the carbonate aquifers, EC values remain at high elevations, and an increase of chlorides has been observed in almost all the wells of this aquifer, e.g., # 120, 118, 18A, etc. [29–31]. In Figure 8, the TDS versus distance from sea graph is shown. The TDS decreases with the increasing distance from the sea. In the north part of the plain, however, it remains high.

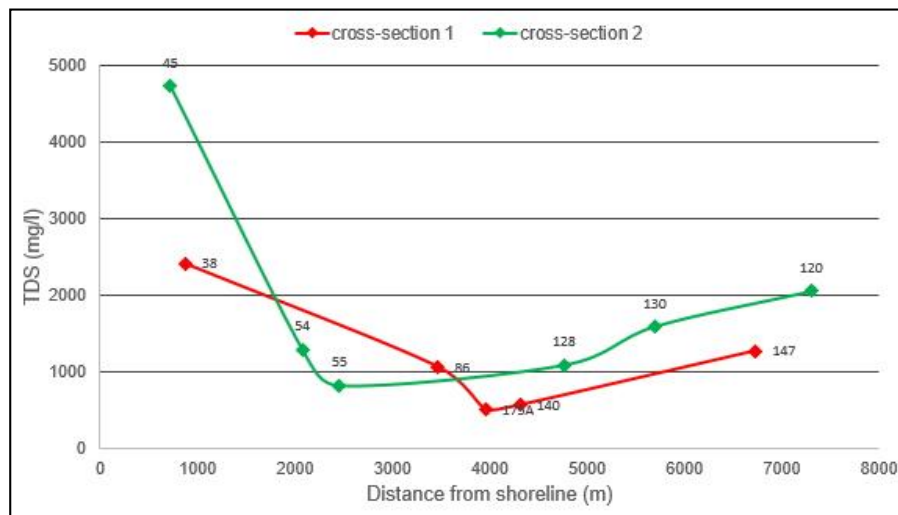


**Figure 8.** Total dissolved solids (TDS) decrease with increasing distance from the sea. In the carbonate located north (wells 120 and 147), it remains high.

All the data mentioned above provide the evidence that modern direct seawater intrusion could occur nowadays only in the carbonate aquifers [56] around the plain but not in the Neogene-Quaternary deposits. In addition, the occurrence of high fluoride concentration in the groundwater [50] indicates rock dissolution, which requires hundreds or thousands of years to be accomplished [58]. Besides, the  $F^-/Cl^-$  molar ratio up to 500 times more than that in modern seawater indicates that there is not an influence of modern seawater. It is very likely the occurrence of palaeo-seawater could explain those values.

#### 5.4. Conceptual Model

Stratigraphic and tectonic factors and Pleistocene sea level fluctuations strongly influenced the hydrogeological regime of the study area. The existence of Pleistocene clays and Pliocene marls has protected, in many places, the Pleistocene and part of the Triassic carbonate aquifers against seawater intrusion. A complex groundwater salinity distribution is encountered, the origin of which is mainly related to the geological history of the area that includes transgressions and regressions of the sea during Pleistocene. The deposition of thick layers of reddish clay in alternation with coarse materials during Pleistocene was crucial [59]. As a sequence, a multi-layered aquifer system was established where the higher-standing aquifer was exposed to seawater intrusion and the lower ones were protected against this phenomenon. During Upper Pleistocene (18 Ka BP), the subjacent

marine strata was freshened up to depths of 100–120 m. The rapid increase of the sea level [41–43] resulted in seawater invading through the lowlands and the buried river valleys, as well as through fractured carbonate formations [60]. In this way, brackish water is encountered 8 to 9 km inland from the present shoreline through Mesozoic carbonates [29,37,49]. After Holocene clay deposition, seawater was entrapped due to the very low permeability of the clay, and the direct seawater intrusion stopped (Figure 9). Moreover, groundwater discharges on the ground surface as an upwards leakage through the preferential flow of clay deposition. Additionally, to the depth, marls protected the overlying aquifers from seawater, which intruded through the carbonate formations underlain marls. Fresh groundwater with fair quality, with EC values between 524 and 1481  $\mu\text{S}/\text{cm}$ , is found at depths between 5 and 90 mbsl in the following wells: # 61, 74, 75, 100, 138, 140, 142, 154, 155, 161', 165, 175, and 176.

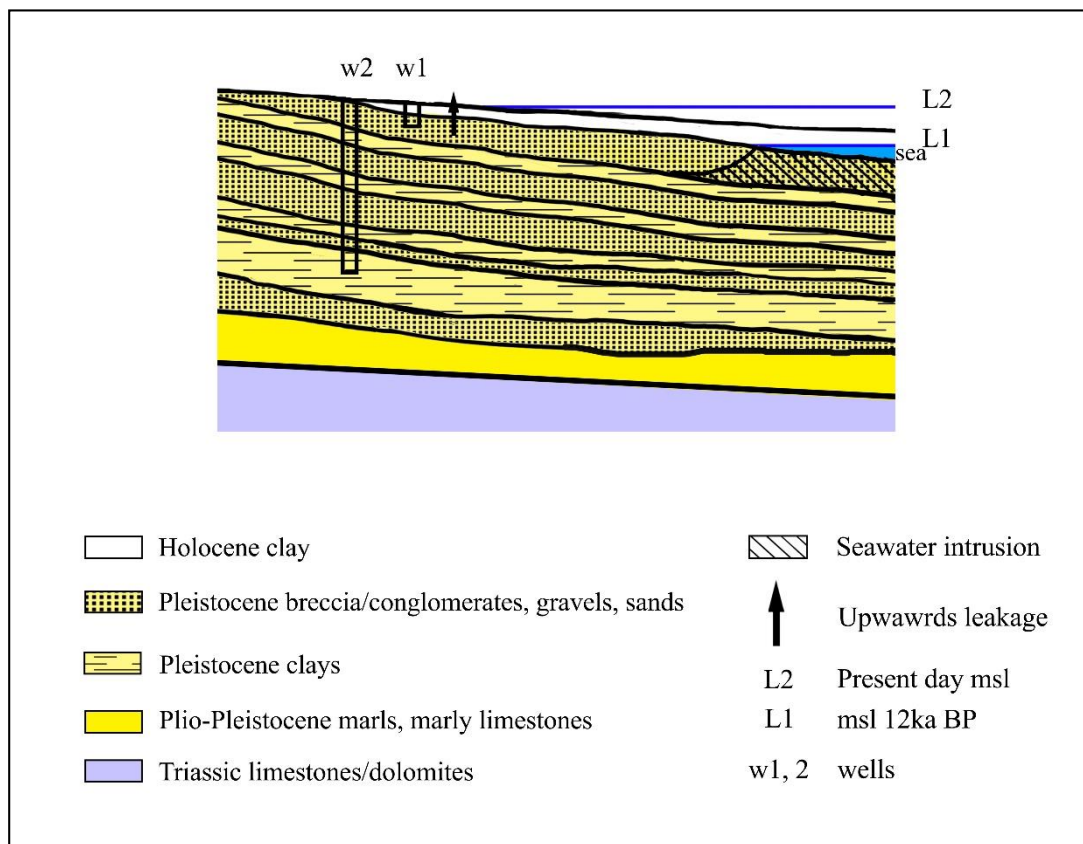


**Figure 9.** Schematic hydrogeological history 12 ka BP and present day. It is very likely that palaeo-seawater was entrapped in the Pleistocene sediments due to Holocene clay deposition.

Fresh groundwater is most likely to be found offshore under the seafloor of the Mediterranean Sea (Eleusis Gulf) (Figure 10). This is an important issue that could be investigated in detail. New ways of expanding the research in groundwater resources under the Eleusis Gulf seafloor could be sought. It is feasible due to the shallow waters of the Eleusis Gulf, which is 34 m in depth at the maximum (mean depth 18 m). In this way, a new perspective on water resource management could emerge. The wide Neogene basin around Attica, Euboea, and Peloponnese at least 15,000  $\text{km}^2$  in total extent presents the same hydrogeological conditions; the same conditions could prevail in many other coastal areas of Greece and even more around the world.

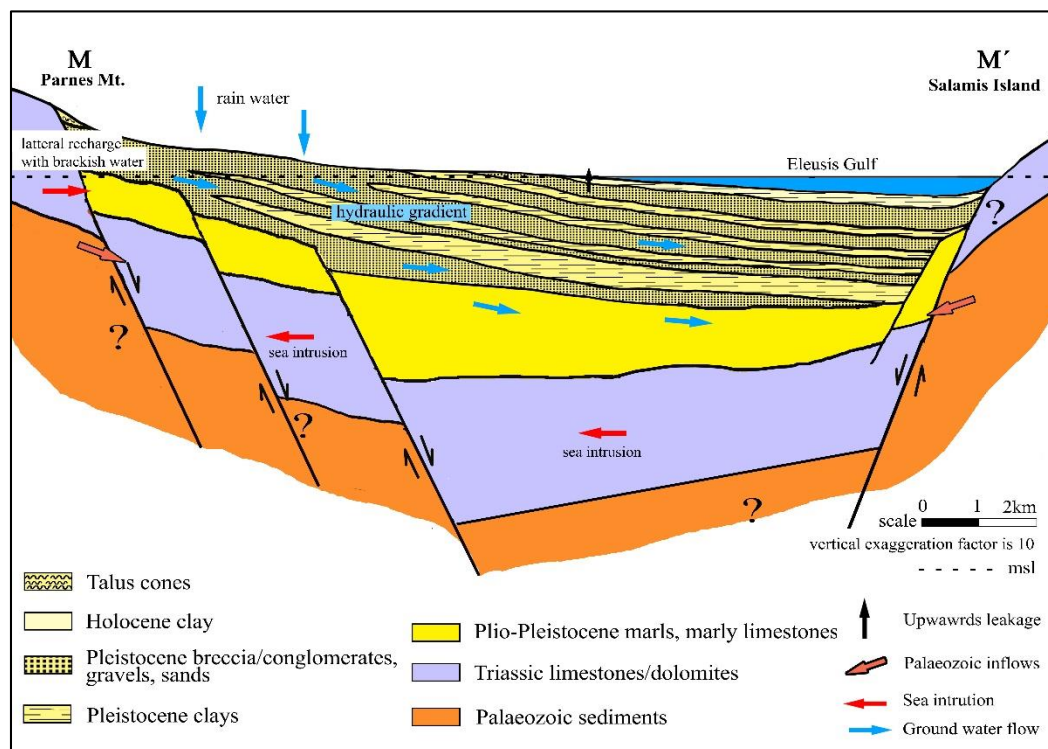


**Figure 10.** Hydrogeological conceptual model of the Thriassion Plain aquifers. Potential fresh groundwater under hydraulic gradient in submarine aquifers below the Eleusis Gulf is shown.

## 6. Conclusions

A completely revised hydrogeological conceptual model was proposed for the Thriassion Plain, West Attica, Greece. We suggest that the saline water hosted in the Neogene-Quaternary coastal aquifers is likely due to seawater entrapment prior Pleistocene-Holocene clay deposition. Due to that, any modern direct-seawater intrusion is precluded. Moreover, an almost stagnant zone is developed within the Pleistocene-Holocene sediments under the coastal area and the Eleusis Gulf seafloor. A minor quantity of groundwater is partly discharged as an upwards leakage through the clay strata, forming wetlands or swamps on the ground surface, whereas the major one moves very slowly southeast. Finally, coupling our data (chemical water analyses and aquifer types) with the existing stratigraphic ones (borehole data), we infer that the submarine fresh water possibly exists in the deeper aquifers beneath the seafloor of the Eleusis Gulf.

**Author Contributions:** Conceptualization, D.H.; methodology, D.H.; formal analysis, D.H.; investigation, D.H., P.M., G.K., and A.A.; resources, D.E.; data curation, P.M. and D.H.; writing—original draft preparation, D.H.; writing—review and editing, D.H., P.M., G.K., and A.A.; visualization, D.H.; supervision, D.H. and A.A.; and project administration, D.H. All authors have read and agreed to the published version of the manuscript.

**Funding:** This research received no funding.

**Acknowledgments:** This study was accomplished at the expense of the Agricultural University of Athens.

**Conflicts of Interest:** The authors declare no conflict of interest.

## References

1. Post, V.E.A. Groundwater Salinization Processes in the Coastal Area of the Netherlands Due to Transgressions during the Holocene. Ph.D. Thesis, Vrije Universiteit, Amsterdam, The Netherlands, 2004; p. 138.
2. Fetter, C.W. *Applied Hydrogeology*, 3rd ed.; Prentice-Hall Inc.: Upper Saddle River, NJ, USA, 1994; p. 600.
3. Fetter, C.W. Intruded and relict groundwater of marine origin. *EOS* **1982**, *63*, 810. [[CrossRef](#)]

4. Custodio, E. Coastal aquifers as important natural hydrogeological structures. In *Groundwater and Human Development*; Bocanegra, M., Massone, M., Eds.; Taylor & Francis: Barcelona, Spain, 2002; pp. 1905–1918.
5. Custodio, E.; Bruggeman, G.A. (Eds.) *Groundwater Problems in Coastal Areas, Studies and Reports in Hydrology*; No. 45, UNESCO; International Hydrological Programme: Paris, France, 1987.
6. Lloyd, J.W.; Heathcote, J.A. *Natural Inorganic Hydrochemistry in Relation to Groundwater*; Clarendon Press: Oxford, UK, 1985; p. 296.
7. Todd, D.K. *Groundwater Hydrology*; John Wiley and Sons: Hoboken, NJ, USA, 1980; Volume 242, pp. 235–247.
8. Todd, D.K. Sea water intrusion in coastal aquifers. *Trans. Am. Geophys. Union* **1953**, *34*, 749–754. [[CrossRef](#)]
9. Bear, J. *Hydraulics of Groundwater*; McGraw-Hill: New York, NY, USA, 1979; p. 567.
10. Freeze, R.A.; Cherry, J.A. *Groundwater*; Prentice-Hall Inc.: Englewood Cliffs, NJ, USA, 1979; 604p.
11. Henry, H.R. Interface between salt water and fresh water in a coastal aquifer. In *Editors Sea Water in Coastal Aquifers*; Cooper, H.H., Jr., Kohout, F.A., Henry, H.R., Glover, R.E., Eds.; U.S. Geological Survey Water Supply: Washington, DC, USA, 1964; pp. C35–C70.
12. Glover, R.E. The pattern of fresh-water flow in a coastal aquifer. In *Sea Water in Coastal Aquifers*; U.S. Geological Survey Water-Supply: Washington, DC, USA, 1964; Volume 1613, pp. 32–35.
13. Hubbert, K.M. The theory of groundwater motion. *J. Geol.* **1940**, *48*, 785–944. [[CrossRef](#)]
14. Herzberg, A. Die Wasserversorgung einiger Nordseebder (The water supply of parts of the North Sea coast in Germany). *Z. Gasbeleucht Wasserversorg* **1901**, *44–45*, 815–819, 842–844.
15. Badon-Ghyben, W. Nota in verband met de voorgenomen putboring nabij Amsterdam (Notes on the probable results of well drilling near Amsterdam). *Tijdschrift van het Koninklijk Instituut van Ingenieurs* **1888**, *9*, 8–22.
16. Cheng, A.H.D.; Ouazar, D. Analytical solutions. In *Seawater Intrusion in Coastal Aquifers—Concepts, Methods and Practices*; Bear, J., Cheng, A.H.D., Sorek, S., Ouazar, D., Herrera, I., Eds.; Kluwer Academic Publishers: Dordrecht, The Netherlands, 1999; pp. 163–191.
17. Meyer, R.; Engesgaard, P.; Sonnenborg, T.O. Origin and Dynamics of Saltwater Intrusion in a Regional Aquifer: Combining 3-D Saltwater Modeling with Geophysical and Geochemical Data. *Water Resour. Res.* **2019**, *5*, 1792–1813. [[CrossRef](#)]
18. Warner, A. On the classification of seawater intrusion. *J. Hydrol.* **2017**, *551*, 619–631. [[CrossRef](#)]
19. Bredehoeft, J.D.; Pinder, G.F. Mass transport in flowing groundwater. *Water Resour. Res.* **1973**, *9*, 194–210. [[CrossRef](#)]
20. Segol, G.; Pinder, G.F.; Gray, W.G. A Galerkin-finite element technique for calculating the transient position of the saltwater front. *Water Resour. Res.* **1975**, *11*, 343–347. [[CrossRef](#)]
21. Custodio, E. Aquifer Overexploitation: What Does It Mean? *Hydrogeol. J.* **2002**, *10*, 254–277. [[CrossRef](#)]
22. Jacob, C.A. Flow of groundwater. In *Engineering Hydraulics*; Rouse, H., Ed.; John Wiley: New York, NY, SUA, 1950; pp. 321–386.
23. Alam, S.M.M. Hydrogeochemical evolution of groundwater of part of Ganges-Meghna Deltaic Plain. *AQUA Mundi* **2010**, *Am03029*, 071–082.
24. Cohen, D.; Person, M.; Wang, P.; Gable, C.W.; Hutchinson, D.; Marksamer, A.; Dugan, B.; Kooi, H.; Groen, K.; Lizarralde, D.; et al. Origin and Extent of Fresh Paleowaters on the Atlantic Continental Shelf, USA. *Ground Water* **2009**, *48*, 143–158. [[CrossRef](#)] [[PubMed](#)]
25. Edmunds, W.M.; Buckley, D.K.; Darling, W.G.; CJMilne, C.J.; Smedley, P.L.; Williams, A.T. Palaeowaters in the aquifers of the coastal regions of southern and eastern England. *Geol. Soc. Lond. Spec. Publ.* **2001**, *189*, 71–92. [[CrossRef](#)]
26. Post, V.; Groen, J.; Kooi, H.; Person, M.; Ge, S.; Edmunds, W.M. Offshore fresh groundwater as a global phenomenon. *Nature* **2013**, *504*, 71–78. [[CrossRef](#)]
27. Jiao, J.J.; Shi, L.; Kuang, X.; Lee, C.M.; Yim, W.W.; Yang, S. Reconstructed chloride concentration profiles below the seabed in Hong Kong (China) and their implications for offshore groundwater resources. *Hydrogeol. J.* **2015**, *23*, 277. [[CrossRef](#)]
28. Burnett, W.C.; Aggarwal, P.K.; Aureli, A.; Bokuniewicz, H.; Cable, J.E.; Charette, M.A.; Kontar, E.; Krupa, S.; Kulkarni, K.M.; Loveless, A.; et al. Quantifying submarine groundwater discharge in the coastal zone via multiple methods. *Sci. Total Environ.* **2006**, *367*, 498–543. [[CrossRef](#)]
29. Hermides, D. Hydrogeological Conditions of the Thriassion Plain Basin with Emphasis on the Geohydraulic Characteristics of the Aquifers and Groundwater Quality. Ph.D. Thesis, Agricultural University of Athens, Athens, Greece, 2018.

30. Kyriazis, D.; Zagana, E.; Stamatis, G.; Fillippidis, F.; Psomiadis, E. Assessment of groundwater pollution in relation to heavy metals of the alluvial aquifer of Thriassion Plain (NW Attica). *Bull. Geol. Soc. Greece* **2013**, *47*, 731–739. [[CrossRef](#)]
31. Christides, A.; Mavrakis, A.; Mitilineou, A. A case of intense seawater intrusion to aquifer of the Thriasio Plain. In Proceedings of the 12th International Conference on Environmental Science and Technology, Dodecanese, Greece, 8–11 September 2011; pp. 152–159.
32. Lioni, A.; Stournaras, G.; Stamatis, G. Degradation of Groundwater quality of Thriassion Plain through Natural Factors and human activity. In Proceedings of the 8th Hydrogeological Congress of Greece, Athens, Greece, 8–10 October 2008; Volume 2, pp. 577–586.
33. Makri, P. Investigating the Pollution from BTEX in the Groundwater of Thriassion Plain. Ph.D. Thesis, University of Athens, Athens, Greece, 2008; p. 260.
34. Papanikolaou, D.; Lekkas, E.; Sideris, C. Geology and tectonics of Western Attica in relation to the 7-9-99 earthquake. *Newsletter of E.C.P.F.E. Counc. Eur.* **1999**, *3*, 30–34.
35. Katsikatsos, G.; Mettos, A.; Vidakis, M.; Dounas, A.; Pomoni, F.; Tsaila-Monopolis, S.; Skourtsi-Koroneou, V. *Geological Map of Greece, in Scale 1:50.000, "Athina-Elefsis" Sheet*; IGME Publication: Athens, Greece, 1986.
36. Zacharias, A.; Sarandakos, K.; Andre, C. *Report on Sample Drilling and Morphotectonics Study in the Area around Koumoundourou Lake*; Technical Report; ELKETHE/IIW: Athens, Greece, 2003.
37. Lionis, M. *Hydrogeological Study of Poikilon Mt*; ASDA: Athens, Greece, 1992.
38. Goumas, G. Investigation of the Structure of Thriassion Plain based on Geophysics. Master's Thesis, University of Athens, Athens, Greece, 2006.
39. Mariolakos, H.; Fountoulis, I.; Sideris, C.; Chatoupis, T. Morphoneotectonic structure of Parnes' Mt of Attica Proceedings of the 9th International Congress, Athens. *Bull. Geol. Soc. Greece* **2001**, *XXIV/1*, 183–190.
40. Dounas, A. The Geology between Megara and Erithres Area. Ph.D. Thesis, University of Athens, Athens, Greece, 1971.
41. Poulos, S.; Ghionis, G.; Maroukian, H. Sea-level rise trends in the Attico–Cycladic region (Aegean Sea) during the last 5000 years. *Geomorphology* **2009**, *107*, 10–17. [[CrossRef](#)]
42. Mariolakos, H.; Theocharis, D. Shifting shores in the Saronic Gulf during the last 18,000 years and the Kychreia paleolimni. In Proceedings of the 9th International Conference, Bulletin of Hellenic Geological Society, Athens, Greece, September 2001; Volume XXXVI 1, pp. 405–413.
43. Lambeck, K. Sea level change and shore-line evolution in Aegean Greece since Upper Palaeolithic time. *Antiquity* **1996**, *70/269*, 588–611. [[CrossRef](#)]
44. Kambouroglou, E. Eretria Paleogeographic and Geomorphological Evolution during Holocene Relationship of the Natural Environment and Ancient Settlements. Ph.D. Thesis, UNKA, Athens, Greece, 1989; p. 493.
45. Kallieris, D. *Our Village*; Cultural Center M. of Aspropyrgos: Aspropyrgos, Greece, 2010; Volume 2, p. 586.
46. Dounas, A.; Panagiotides, G. *Precursor Report on the Hydrogeological Conditions of Thriassion*; Institute of Geology and Subsurface Research: Athens, Greece, 1964.
47. Paraschoudes, B. *Hydrogeological Study of Western Attica*; Agricultural Ministry: Athens, Greece, 2002.
48. Kounis, G.; Simos, N. *Hydrogeological Research of the Aquifers of Thriassion Plain, for the Water Supply of Hellenic Refinery*; IGME: Athens, Greece, 1990; p. 38.
49. Hermides, D. Geochemical evolution of the Thriassion Plain groundwaters, Attica, Greece. *Environ. Monit. Assess* **2020**, *192*, 561. [[CrossRef](#)]
50. Hermides, D.; Stamatis, G. Origin of halogens and their use as environmental tracers in aquifers of Thriassion Plain, Attica, Greece. *Environ. Earth Sci.* **2017**, *76*, 306. [[CrossRef](#)]
51. Hopkins, T.S.; Coachman, L.K.; Edwards, R.F. Seasonal change in Elefsis Bay, Greece. *Rapp. Comm. Int. Mer. Medit.* **1976**, *23*, 77–80.
52. Friligos, N.; Barbetseas, S. Water masses and eutrophication in a Greek anoxic marine bay. *Toxicol. Environ. Chem.* **1990**, *28*, 11–23. [[CrossRef](#)]
53. Theis, C.V. The relation between the lowering of the piezometric surface and the rate and duration of discharge of a well using ground water storage. *Trans. Am. Geophys. Union* **1935**, *16*, 519–524. [[CrossRef](#)]
54. Cooper, H.H.; Jacob, C.E. A generalized graphical method for evaluating formations constants and summarizing well-field history. *Trans. Am. Geophys. Union* **1946**, *27*, 526–534. [[CrossRef](#)]
55. Neumann, S.P. Analysis of pumping test data from anisotropic unconfined aquifers considering delayed gravity response of the water table. *Water Resour. Res.* **1975**, *11*, 329–342. [[CrossRef](#)]

56. Papadopulos, I.S.; Cooper, H.J. Drawdown in a well of large diameter. *Water Resour. Res.* **1967**, *3*, 241–244. [[CrossRef](#)]
57. Schafer, D.C. *Casing Storage can Affect Pumping Test Data*; Johnson Drillers' Journal, Jan/Feb, Johnson Division, UOP Inc.: St. Paul, MI, USA, 1978.
58. Edmunds, W.M.; Smedley, P.L. Fluoride in natural waters. In *Essentials of Medical Geology*; Selinus, O., Ed.; Springer: Enschede, The Netherlands, 2013; pp. 311–336.
59. Tal, A.; Weinstein, Y.; Wollman, S.; Goldman, M.; Yechieli, Y. The Interrelations between a Multi-Layered Coastal Aquifer, a Surface Reservoir (Fish Ponds), and the Sea. *Water* **2018**, *10*, 1426. [[CrossRef](#)]
60. Bakalowicz, M. Coastal Karst Groundwater in the Mediterranean: A Resource to Be Preferably Exploited Onshore, Not from Karst Submarine springs. *Geosciences* **2018**, *8*, 258. [[CrossRef](#)]

**Publisher's Note:** MDPI stays neutral with regard to jurisdictional claims in published maps and institutional affiliations.



© 2020 by the authors. Licensee MDPI, Basel, Switzerland. This article is an open access article distributed under the terms and conditions of the Creative Commons Attribution (CC BY) license (<http://creativecommons.org/licenses/by/4.0/>).